Kinetics of an optically pumped metastable Ar laser

Jiande Han, Michael C. Heaven, Emory University, Atlanta, GA 30322.
Gordon D. Hager, Air Force Institute of Technology; Dayton, OH 45433.
George B. Venus, Leonid B. Glebov, The College of Optics & Photonics, University of Central Florida, Orlando, FL 32816.

ABSTRACT

In recent studies, an optically pumped Ar*/He laser has been demonstrated using the Ar $4p[1/2]_1 \rightarrow 4s[3/2]_2$ transition at 912.55 nm. Time-resolved data for this system, recorded using CW laser excitation and pulsed discharge production of Ar* $4p[3/2]_2$, yielded laser output pulses that were of unexpectedly short duration. It was speculated that radiative relaxation from the upper laser level to the $4s[3/2]_1$ state (607 cm^{-1} above $4s[3/2]_2$) caused termination of the laser pulse. In the present study this hypothesis has been tested by observing the energy transfer kinetics of the $4s[3/2]_2$ and $4s[3/2]_1$ states in Ar/He gas mixtures. Following pulsed laser excitation out of $4s[3/2]_2$, population recovery was observed on a μs time scale. Energy transfer from $4s[3/2]_1$ to $4s[3/2]_2$, induced by collisions with He, was characterized. The rate constant was found to be $(1.0\pm0.5)\times10^{-13}$ cm^3 s^{-1}. These observations confirmed that radiative transfer to $4s[3/2]_1$ was responsible for the short duration laser pulses. Modeling of a fully CW optically pumped Ar* laser shows that radiative transfer to $4s[3/2]_1$ reduces the number density of the Ar* atoms involved in lasing, but is otherwise benign.

INTRODUCTION

Hybrid laser systems consisting of a gaseous lasing medium driven by a solid-state optical pump source offer significant technological advantages for certain high-power applications. In principle, this approach can be used to generate high-power (>100 kW) laser beams that have excellent beam quality and atmospheric transmission properties. Diode pumped alkali lasers (DPAL's) are the most extensively developed hybrid systems at the present time[1-4].

In recent years, the possibility of using rare gases (Ne, Ar, Kr and Xe) in metastable electronically excited states as laser media has been examined[5-7]. An advantage of the rare gas systems, as compared to DPAL's, is that the lasing medium is chemically inert. The rare gas metastables are produced by promoting one of the outermost *p*-electrons to the first unoccupied *s*-orbital ($np^5(n+1)s \leftarrow np^6$). In the following we denote electronically excited Rg atoms by Rg*. The lowest energy triplet state of the $np^5(n+1)s$ configuration, $^3P_2$ (= $(n+1)s[3/2]_2$ in Racah notation, where the subscripted number gives the electronic angular momentum) is long-lived. This state is metastable because the radiative transition back to the $^1S_0$ ground state is electric dipole forbidden. Many of the $np^5(n+1)p \leftarrow np^5(n+1)s$ absorption transitions of the metastable rare gases are strongly allowed, with very similar characteristics to the $p \leftarrow s$ transitions used in the optically pumped alkali metal lasers[8]. However, the energy level pattern is more complex for Rg* as the outermost electron sits above an open-shell $Rg^+(np^5)$ ionic core. As a consequence, there are four states that correlate with $np^5(n+1)s$ and ten states that correlate with $np^5(n+1)p$. The energy levels that are of importance for the optically pumped laser are shown in Fig. 1. This diagram is for Ar*, but the energy levels for Ne*, Kr* and Xe* all have the same ordering.

High Energy/Average Power Lasers and Intense Beam Applications VII, edited by
Steven J. Davis, Michael C. Heaven, J. Thomas Schriempf, Proc. of SPIE Vol. 8962, 896202
 · doi: 10.1117/12.2045164

The viability of optically pumped Rg* lasers has been explored in two recent studies[5,6]. The initial demonstration was performed using a pulsed electrical discharge to generate Rg* in the presence of a relatively high pressure of a buffer gas (0.5-2.0 atm). The buffer gas, usually He, was needed for transfer of population from the optically pumped level to the upper laser level. Pulsed optical excitation was used to induce lasing from Rg*/He mixtures with Rg=Ne, Ar, Kr, and Xe. In addition, lasing from pure Ar was observed at a total pressure of 1 atm.

Laser demonstration experiments that employ pulsed laser excitation benefit from very high instantaneous intensities (10 MW cm^{-2} is easily achieved) and the short time-scale over which the kinetics can develop. Consequently, the question of whether an Rg* laser could be excited using a CW diode pump has been examined[6]. The experiments carried out to date have focused on Ar* in He. A narrow linewidth diode laser was custom made for this project. The laser provided powers up to 7.5 W with a linewidth of 20 pm. The tuning range was centered on the Ar* $4p[5/2]_3 \leftarrow 4s[3/2]_2$ transition at 811.754 nm. A pulsed DC glow discharge (parallel plates) was used to generate Ar* in the presence of 420 Torr of He. The electrical power supply available for these experiments was configured to generate voltage pulses of 0.5 to 20 μs duration. With the pump laser tuned on-resonance, Ar* laser output pulses were observed for every discharge pulse. Surprisingly, the duration of the output pulse (typically around 100-200 ns) was found to be much shorter than the voltage pulse applied to the discharge plates. In the present study we examine the question of why the lasing pulse terminated before the end of the discharge pulse. The results yield valuable insights regarding the kinetics of the Ar* laser.

EXPERIMENTAL

The apparatus used to investigate optically pumped Ar* is shown in Fig. 2. As the description of this system has been presented in ref.[6], the information given here is focused on the details of relevance to the kinetic measurements. Parallel plate electrodes were used to generate a glow discharge in Ar/He mixtures. In most experiments, the electrodes were square 2.5x2.5 cm stainless steel plates separated by 0.5 cm. One plate was held at ground while a pulsed negative voltage of up to 2500 V was applied to the opposing electrode. A few experiments were performed using a dielectric barrier discharge. This discharge mode was obtained by covering one of the electrodes by a 0.8 mm thick sheet of alumina. The optical configuration shown in Fig. 2 was used for laser demonstration experiments. Measurements of the absorption of the diode laser were made with the mirror shown on the left hand side of the figure replaced by a beam attenuator and a photodiode.

Pulsed laser pump - probe experiments were carried out to observe the kinetics of population transfer. The experimental set up used for these measurements is shown in Fig. 3. Wavelength tunable excitation pulses were provided by an Nd/YAG pumped OPO (FWHM linewidth 1 cm^{-1}, 10 ns pulse duration) and an excimer pumped dye laser (linewidth 0.3 cm^{-1}, 10 ns pulse duration). The firing of the discharge and the two pulsed lasers was controlled by precision pulse delay generators. Computer control of the delay generators facilitated the smooth variation of the delay between the pump and probe laser pulses. Kinetic measurements were carried out with fixed delays between the beginning of the discharge pulse and the pump laser pulse. Fluorescence produced by either the discharge, pump laser or probe laser was observed along an axis that was perpendicular to the collinear laser beams. The fluorescence was dispersed by a small monochromator (0.2 m) and detected by a photomultiplier tube.

The mechanical pump used for the vacuum system produced an ultimate vacuum of less than 10 mTorr. Ultra high purity argon and helium were used in the experiments. These reagents were flowed continuously through the discharge region, and the gas composition was defined by feedback controlled metering valves on each of the gas inlet lines. A throttle valve on the evacuation line was used to control the total pressure, which was measured by a capacitance manometer. Nitrogen cold traps were used on both the inlet and outlet sides of the discharge chamber in order to further purify the gases and prevent contamination from back-streaming pump oil vapor.

RESULTS AND DISCUSSION

Fig. 4 shows results obtained using the apparatus shown in Fig. 2. The upper trace shows the absorption of the output from the CW diode laser, resulting from discharge pulse generation of Ar* $4s[3/2]_2$. For this measurement the diode laser power was attenuated to the mW range, in order to minimize optical pumping effects. Note that the metastables persisted for a several μs beyond the termination of the voltage pulse. This measurement was made for a gas mixture of 78 mTorr of Ar in 522 Torr of He. The lower trace shows the lasing performance of the same gas mixture, excited using a diode laser power of approximately 6 W. Here it can be seen that the laser pulse occurs very early in the discharge pulse, and terminates within 150 ns. This suggests that the population of lower laser level is being depleted by the optical pumping process, under conditions where the repopulation by relaxation and discharge excitation is too slow to be competitive.

Further evidence of bleaching by the pump laser was provided by studies of the dielectric barrier discharge system. Fig. 5 shows pump laser absorption measurements for a mixture of 26 Torr of Ar in 274 Torr of He. Traces are shown for laser powers of 1, 1.8, 2.6 and 3.8 W. The discharge was operated at -1500 V, with an applied voltage duration of 20 μs. These data clearly demonstrate that the absorption was bleached by the pump laser, and that the rate of bleaching was proportional to the pump laser power.

The energy level diagram of Fig. 1 provides a possible explanation for these observations. The optical selection rule $\Delta J=0, \pm 1$ (where J is the electronic angular momentum) are such that the upper level of the pump transition, $4p[5/2]_3$, can only radiate back to the $4s[3/2]_2$ level. However, following collisional relaxation to the $4p[1/2]_1$ upper laser level, this state can radiate back to the $4s[3/2]_2$ and $4s[3/2]_1$. The Einstein coefficients for these transitions are 1.89×10^7 and 0.54×10^7 s^{-1}, respectively. Hence, 22% of the population from $4p[1/2]_1$ will radiate back to $4s[3/2]_1$ if the system is not lasing. The optical bleaching can be accounted for by radiative transfer to $4s[3/2]_1$ if repopulation of the $4s[3/2]_2$ level (by collisional relaxation and discharge excitation) is relatively slow.

Time resolved pump-probe measurements (apparatus shown in Fig. 3) were made to examine the kinetics of the $4s[3/2]_2$ and $4s[3/2]_1$ levels. These experiments relied on laser induced fluorescence (LIF) detection of the populations of interest. Strong, fully allowed transitions were used in these measurements, and in all cases the radiative decay rates of the upper level for the probe transition (greater than 10^7 s^{-1}), were far faster than the decay processes characterized (typically in the μs range). Hence, the kinetics of the LIF detection process could be safely ignored in the analyses of the kinetic data.

Repopulation of the $4s[3/2]_2$ level was observed by using the first laser pulse to strongly excite the $4p[5/2]_3 \leftarrow 4s[3/2]_2$ transition, thereby significantly depleting the population of the lower level. A probe laser, tuned to the $4p[3/2]_2 \leftarrow 4s[3/2]_2$ transition at 763.51 nm was used to track the lower level population. These measurements were made 10 μs after the termination of the voltage pulse. A representative result is shown in Fig. 6, for a mixture 8 Torr of Ar in 442 Torr of He. Zero time in this trace is for the synchronous firing of both lasers, and negative delays are for the probe laser firing before the pump laser (to establish the baseline signal level). Delay scans were recorded with the pump laser on- and -off resonance. Subtraction of these signals was used to remove any fluctuation in the baseline. Fig 6. shows that the population in $4s[3/2]_2$ was promptly depleted by the pump laser, and recovered with an approximately exponential time dependence. The time constant for this process was in the range of 0.5 - 1.5 μs. Note also that the population did not recover to the value prior to the pump pulse, indicating that there was population loss to other states. Overall, these observations were consistent with rapid radiative transfer of about 10% of the $4s[3/2]_2$ population to $4s[3/2]_1$, followed by a much slower collisional relaxation back to $4s[3/2]_2$. The loss of population in this cycle was consistent with radiative decay of $4s[3/2]_1$ back to the $3p^6\ ^1S_0$ ground state (see below).

This cascade model was tested by examining the transient population in $4s[3/2]_1$. These post-discharge measurements also used pulsed excitation of the $4p[5/2]_3 \leftarrow 4s[3/2]_2$ transition, with the probe laser now tuned to the $4p[1/2]_0 \leftarrow 4s[3/2]_1$ transition at 751.47 nm. Fig. 7 shows representative examples of the time resolved $4s[3/2]_1$ signals. Here it is evident that the decay rate for $4s[3/2]_1$ was very similar to the recovery rate for $4s[3/2]_2$. As these measurements were performed in He/Ar mixtures, both of these collision partners could contribute to the relaxation process. To obtain relaxation rate constants, measurements were preformed where the partial pressure of one gas was varied, while that of the other held constant. Variation of the Ar pressure over the range 7 - 32 Torr, in the presence of 400 Torr of He, produced no measureable effect on the decay rate. Conversely, variation of the He pressure over the range of 150 - 450 Torr, with the pressure of Ar held at 20 Torr, yielded a linear dependence of the decay rate on the He pressure. Fig. 8 shows the decay rate plotted as a function of He pressure. A liner fit to these data yielded a population transfer rate constant of $k^{He}=(1.0\pm0.5)\times10^{-13}$ cm^3 s^{-1}. We estimate that the temperature of the gas was approximately 300 K. As the relaxation by Ar appeared to be insignificant, the zero He pressure intercept of this plot gives an estimate of 5.7×10^5 s^{-1} for the spontaneous decay rate for the $4s[3/2]_1$ state. This is orders of magnitude slower than the radiative decay rate (1.2×10^8 s^{-1}) due to radiation trapping in the high density of ground state Ar.

The slow transfer of population from $4s[3/2]_1$ to $4s[3/2]_2$ could account for the short pulse duration of the CW pumped laser experiments[6], but there were additional factors that needed to be considered. The first series of kinetic measurements were made after the termination of the discharge pulse, while the CW pump laser kinetics were observed during the applied voltage. Consequently, the latter could be influenced by super-elastic electron collisions and discharge repopulation of the $4s[3/2]_2$ state. In an attempt to test for transfer induced by electrons, pump-probe measurements for the $4s[3/2]_1$ state population were performed with the pump laser firing after 0.5 μs in a 1μs voltage pulse, and after 1.5 μs in a 4 μs pulse. The decay rates obtained were consistent with the post-discharge measurements, indicating that repopulation of $4s[3/2]_2$ was dominated by collisional relaxation.

It was somewhat surprising to find that discharge excitation of $4s[3/2]_2$ was relatively slow in the middle of a 1 μs applied voltage pulse. To learn more about the discharge kinetics, time resolved measurements of the applied voltage, discharge current and discharge-excited Ar* emission

signals were made. The discharge current was deduced by observing the voltage across a 0.5 Ω resistor in the path to ground. Fig. 9 shows results for a mixture of 17 Torr of Ar in 300 Torr of He. Applied voltages of -900, -1300, -1700, -2100, and -2500 V were examined. The middle trace of Fig. 9 shows the discharge-excited $4p[5/2]_3 \rightarrow 4s[3/2]_2$ emission. Note that the emission pulses appear some 200 - 300 ns after the applied voltage, and that the delay between these events decreases with increasing voltage. This behavior correlates with the discharge current (lower trace in Fig. 9). It is apparent that the Ar* emission occurred early in the gas break-down process, and decayed to a low level within an interval of approximately 100 ns. This indicates that the majority of the Ar* metastables produced in our pulsed glow discharge were formed during the initial gas break-down, and that the power supply storage capacitor was discharged on the 100's of ns timescale. These observations explain why discharge generation of $4s[3/2]_2$ could not sustain optically pumped laser pulse durations beyond 200 ns in our CW pump / pulsed discharge laser experiments (c.f., Fig. 4).

COMPUTATIONAL MODELING

Modeling of an optically pumped Ar*/He laser was carried out to examine the impact of radiative transfer of population to the $4s[3/2]_1$ level. The model, based on the equations developed by Zameroski et al.[4] for DPAL systems, considers a steady-state CW device. In the following, the levels of importance for the Ar* laser are labeled as $1 \equiv 4s[3/2]_2$, $2 \equiv 4s[3/2]_1$, $3 \equiv 4p[1/2]_1$, and $4 \equiv 4p[5/2]_3$. The total population within these four levels ($n_{Total}=n_1+n_2+n_3+n_4$) was held constant. The steady-state kinetic equations for this system are given by,

$$\frac{dn_1}{dt} = 0 = \left(\frac{-\Omega}{h\nu_{41}}\right) + \sigma_{31}(n_3 - (3/5)n_1)\left(\frac{\Psi}{h\nu_{31}}\right) + \gamma_{21}(n_2 - (3/5)n_1 Exp[-\theta_{21}]) + n_4\Gamma_{41} + n_3\Gamma_{31} \quad (1)$$

$$\frac{dn_2}{dt} = 0 = n_3\Gamma_{32} - \gamma_{21}(n_2 - (3/5)n_1 Exp[-\theta_{21}]) \quad (2)$$

$$\frac{dn_3}{dt} = 0 = -\sigma_{31}(n_3 - (3/5)n_1)\left(\frac{\Psi}{h\nu_{31}}\right) + \gamma_{43}(n_4 - (7/3)n_3 Exp[-\theta_{43}]) - n_3\Gamma_{32} - n_3\Gamma_{31} \quad (3)$$

with n_4 determined by the conservation of total population. In the above equations, Ω is the circulating optical pump intensity within the laser cavity, Ψ is the circulating laser intensity, ν_{ij} is the frequency for the transition between states i and j, σ_{ij} is the absorption cross section for the transition between states i and j, and γ_{ij} is the collisional transfer rate for relaxation for upper state i to lower state j. The endothermic reverse transfer rates are obtained from detailed balance. Hence, $\theta_{ij}=(E_i-E_j)/k_bT$. Lastly, the radiative decay rates (Einstein coefficients) are specified as Γ_{ij}. The device parameter values chosen for this model were relevant to the recent CW laser demonstration experiments of Rawlins et al. (paper 8962-2 of this volume). The optical cavity consisted of a total reflector and an output coupler with a reflectivity of 15%. The path length for the active medium was 1.9 cm. The gas mixture was set to 15 Torr of Ar in 754 Torr of He. Using the present rate constant data for transfer from state 2 to state 1, and the data of Han and Heaven[9] for 4 to 3 transfer, the rates were set to $\gamma_{43}=3.1\text{x}10^8$ and $\gamma_{21}=2.4\text{x}10^6$ s^{-1}. The radiative decay rates, taken from the NIST electronic database[10], were $\Gamma_{41}=3.3\text{x}10^7$, $\Gamma_{32}=5.43\text{x}10^6$ and $\Gamma_{31}=1.89\text{x}10^7$ s^{-1}. Taking into account both the pressure and Doppler broadening, the line center

absorption cross sections were σ_{31}=3.7x10^{13} and σ_{41}=5.2x10^{-13} cm^2. With the assumption of a 2.5% round trip cavity loss for the lasing radiation, the threshold gain for this system was 0.53 cm^{-1}. Simulations of the absorbed intensity and laser output intensity verses the pump intensity were made with and without radiative transfer to level 2 to assess the impact of this channel. A total Ar* number density of 1x10^{13} cm^{-3} was assumed for these calculations. The results are shown in Fig's 10a and 10b. Comparing these traces it is evident that radiative transfer to level 2 ($4s[3/2]_1$) reduces both the pump intensity absorbed and the lasing intensity. The steady-state populations show that both effects are caused by the build-up of population in level 2. For example, with an input power of 600 W cm^{-2} the calculation indicates that more than half of the total Ar* is in state 2 (n_2=5.6x10^{12} cm^{-3}). A calculation with n_{Total}=4.4x10^{12} cm^{-3} and the radiative transfer to level 2 suppressed yielded absorption and laser intensity curves that were very close to those of Fig. 9a. At 600 W cm^{-2} of input intensity the absorbed and laser intensities were 159 and 102 W cm^{-2}, respectively. This indicates that the primary effect of the radiative transfer is to reduce the number density of the Ar* atoms that can participate in the lasing process. Note that there will be some mitigating effects in a fully CW laser system. The present model does not include discharge repopulation of $4s[3/2]_2$ or re-absorption of the $4p[1/2]_1 \rightarrow 4s[3/2]_1$ radiation. The calculations indicate that the effects of population sequestered in the $4s[3/2]_1$ state can be compensated for by increasing the gain length and / or increasing the total Ar* population.

ACKNOWLEDGEMENTS

This work was supported by the Joint Technology Office through the Air Force Office of Scientific Research (AFOSR) under contract FA9550-13-1-0002.

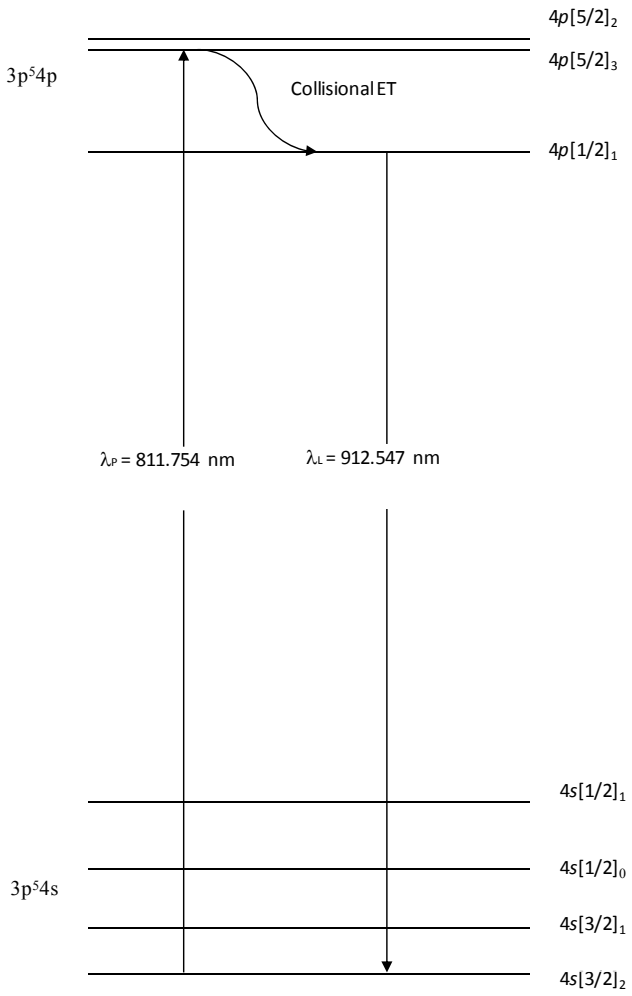

Figure 1. Partial energy level diagram for the states of Ar*

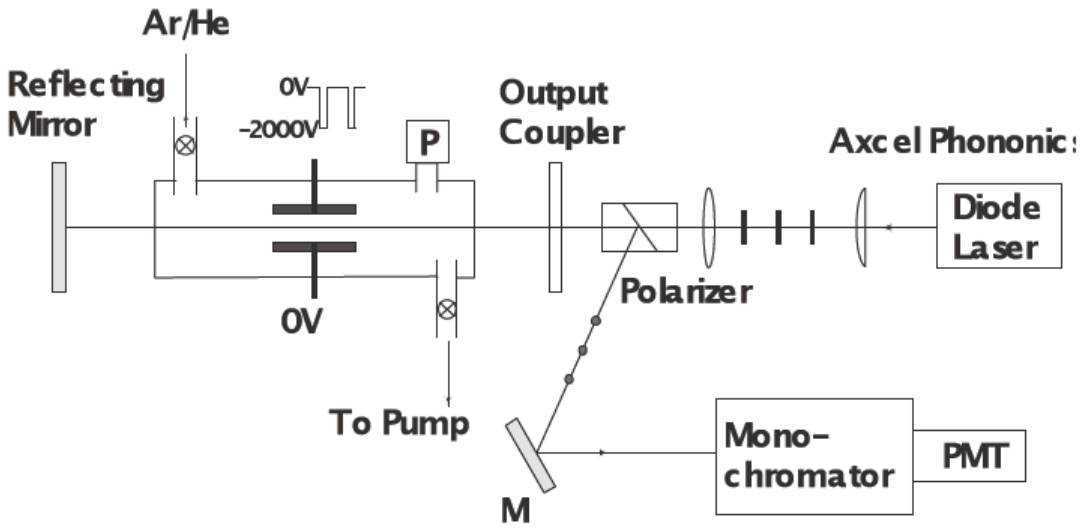

Figure 2. Apparatus used for CW optical pumping of Ar* in a pulsed discharge

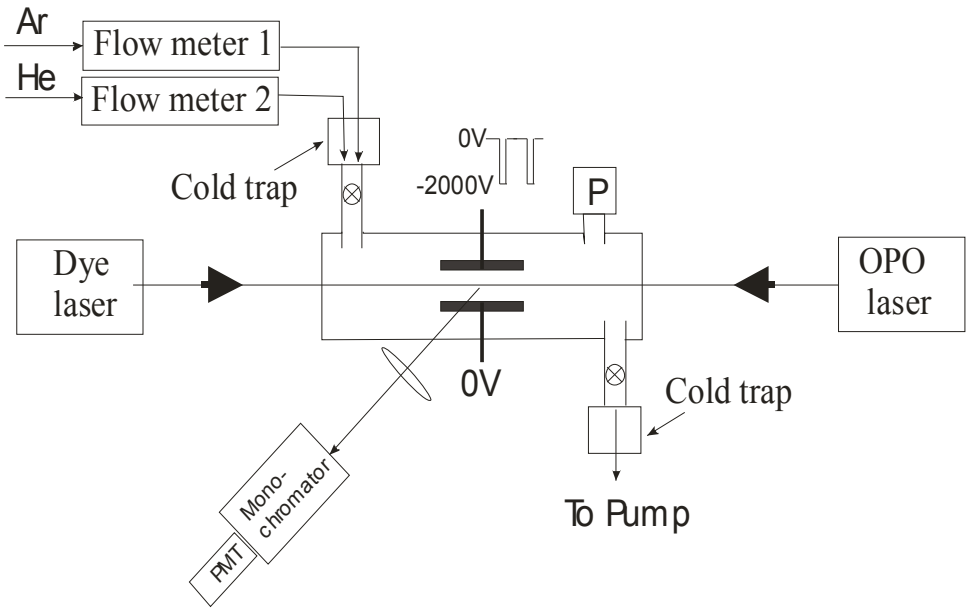

Figure 3. Apparatus used for pump-probe kinetic measurements for Ar* metastables in He.

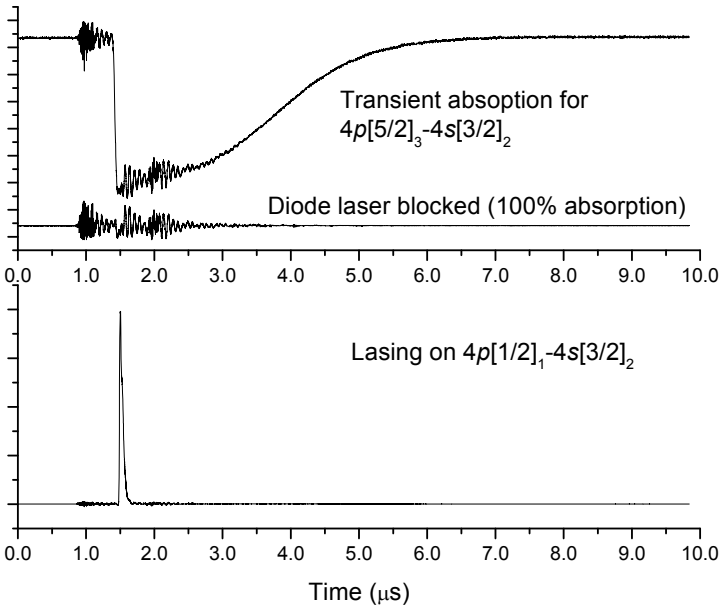

Figure 4. Transient absorption and lasing signals observed in a discharge excited mixture of Ar and He.

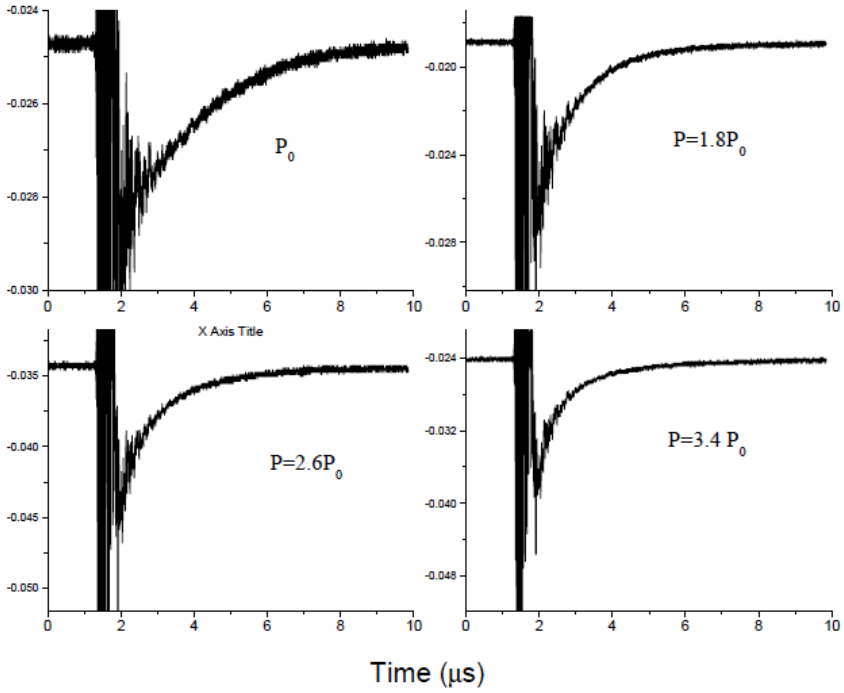

Figure 5. Transient absorption signals observed in a discharge excited mixture of Ar and He. A dielectric barrier discharge was used for these measurements.

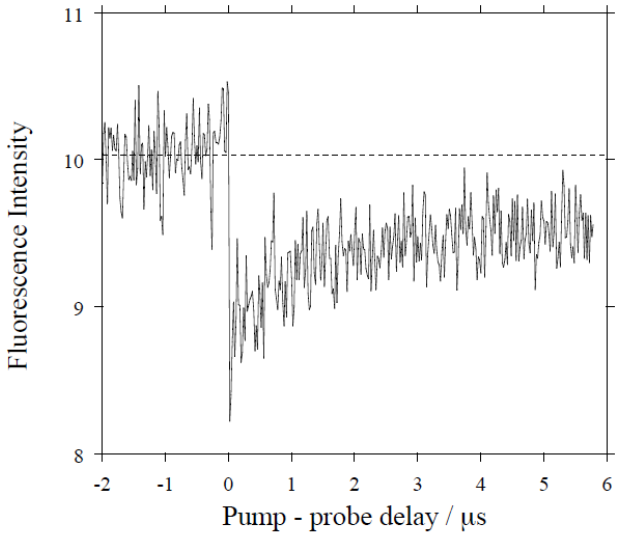

Figure 6. Transient loss of population from the $4s[3/2]_2$ level induced by pulsed optical excitation of the $4p[5/2]_3 \leftarrow 4s[3/2]_2$ transition

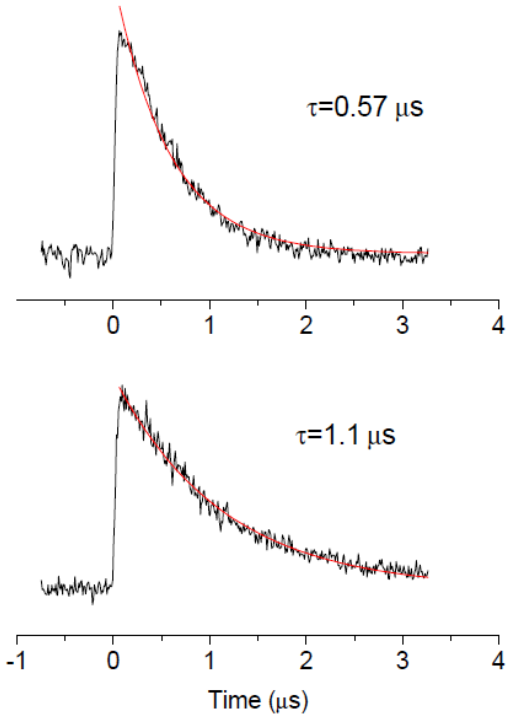

Figure 7. Transient population of the $4s[3/2]_1$ level induced by pulsed optical excitation of the $4p[5/2]_3 \leftarrow 4s[3/2]_2$ transition. P(He)=400 and 130 Torr for the upper and lower traces, respectively.

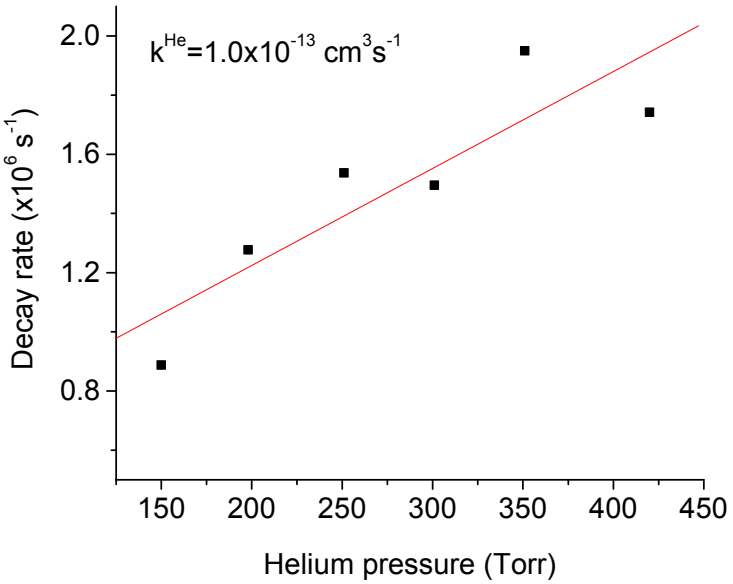

Figure 8. The Ar 4p[3/2]$_1$ population decay rate plotted as a function of He pressure.

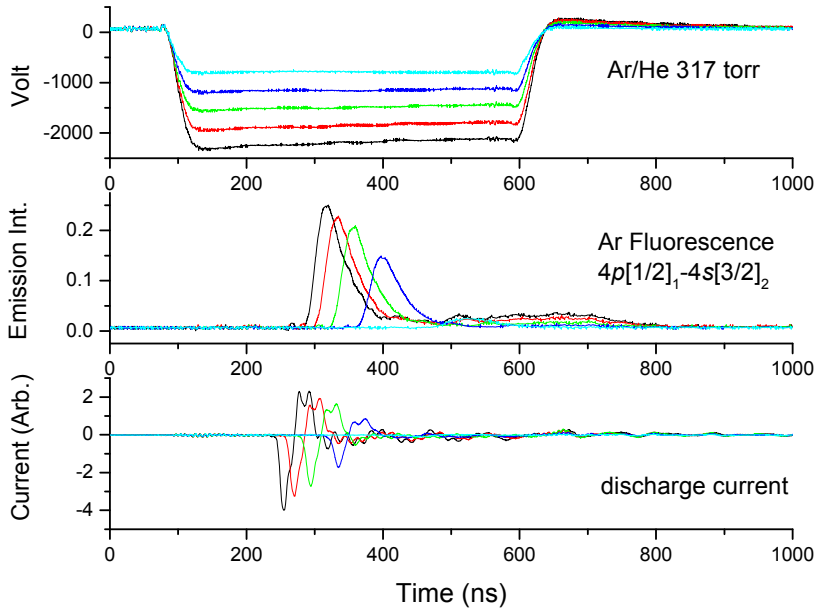

Figure 9. Time dependent characteristics of the pulsed Ar/He discharge for 17 Torr of Ar in 300 Torr of He.

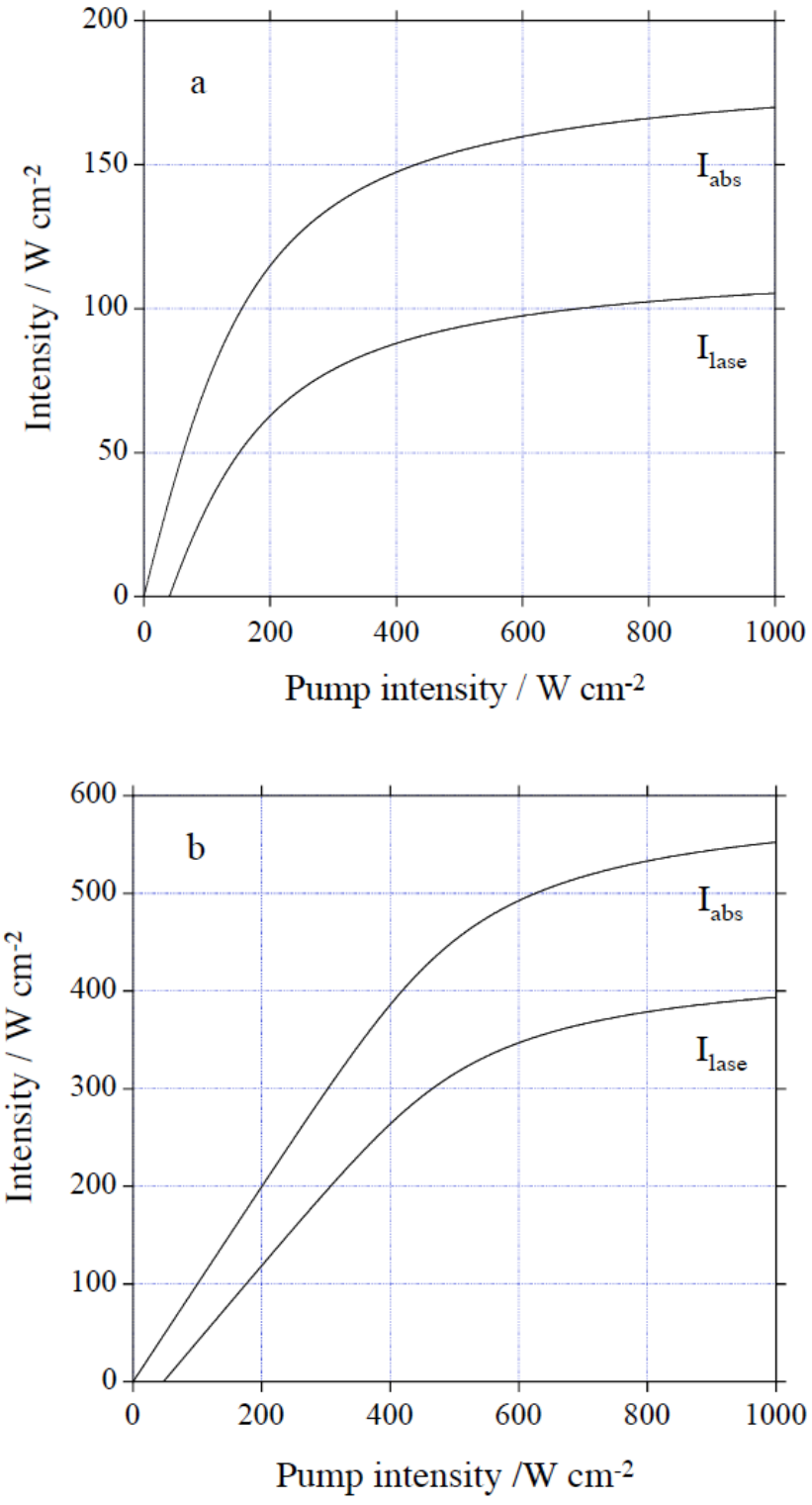

Figure 10. Model calculations for an optically pumped Ar*/He laser. Plot 10a shows the results for Γ_{32}= 5.4x10^{6} s^{-1}. Plot 10b is for Γ_{32}= 0. See text for details.

REFERENCES

(1) Zhdanov, B.V.; Knize, R.J. "Review of alkali laser research and development", *Opt. Eng.* **2013**, *52*, 021010/021011-021010/021018.

(2) Gao, F.; Chen, F.; Xie, J.J.; Li, D.J.; Zhang, L.M.; Yang, G.L.; Guo, J.; Guo, L.H. "Review on diode-pumped alkali vapor laser", *Optik* **2013**, *124*, 4353-4358.

(3) Bogachev, A.V.; Garanin, S.G.; Dudov, A.M.; Yeroshenko, V.A.; Kulikov, S.M.; Mikaelian, G.T.; Panarin, V.A.; Pautov, V.O.; Rus, A.V.; Sukharev, S.A. "Diode-pumped cesium vapour laser with closed-cycle laser-active medium circulation", *Quantum Electronics* **2012**, *42*, 95-98.

(4) Zameroski, N.D.; Hager, G.D.; Rudolph, W.; Hostutler, D.A. "Experimental and numerical modeling studies of a pulsed rubidium optically pumped alkali metal vapor laser", *J. Opt. Soc. Am. B* **2011**, *28*, 1088-1099.

(5) Han, J.; Heaven, M.C. "Gain and lasing of optically pumped metastable rare gas atoms", *Opt. Lett.* **2012**, *37*, 2157-2159.

(6) Han, J.; Glebov, L.; Venus, G.; Heaven, M.C. "Demonstration of a diode-pumped metastable Ar laser", *Opt. Lett.* **2013**, *38*, 5458-5461.

(7) Kabir, M.H.; Heaven, M.C. "Energy Transfer Kinetics of the np5(n + 1)p Excited States of Ne and Kr", *J. Phys. Chem. A* **2011**, *115*, 9724-9730.

(8) Setser, D.W.; Dreiling, T.D.; Brashears, H.C., Jr.; Kolts, J.H. "Analogy between electronically excited state atoms and alkali metal atoms", *Faraday Discuss. Chem. Soc.* **1979**, *67*, 255-272.

(9) Han, J.; Heaven, M. C. "Relaxation of metastable states of Ar by collisions with He", *work in progress* **2014**.

(10) Kramida, A., Ralchenko, Yu., Reader, J., and NIST ASD Team (2013). NIST Atomic Spectra Database (ver. 5.1), [Online]. Available: http://physics.nist.gov/asd. National Institute of Standards and Technology, Gaithersburg, MD.